air

MDPI

Article

Physico-Chemical Characterisation of Particulate Matter and Ash from Biomass Combustion in Rural Indian Kitchens

Gopika Indu [1,2,*], Shiva Nagendra Saragur Madanayak [1] and Richard J. Ball [3]

[1] Department of Civil Engineering, Indian Institute of Technology Madras, Chennai 600036, India; snagendra@iitm.ac.in
[2] HEAL Global Research Centre, Faculty of Health, University of Canberra, Canberra, ACT 2617, Australia
[3] Centre for Integrated Materials, Processes & Structures (IMPS), Department of Architecture & Civil Engineering, University of Bath, Bath BA2 7AY, UK; r.j.ball@bath.ac.uk
* Correspondence: ce18d405@smail.iitm.ac.in

Abstract

In developing countries, indoor air pollution in rural areas is often attributed to the use of solid biomass fuels for cooking. Such fuels generate particulate matter (PM), carbon monoxide (CO), carbon dioxide (CO_2), polyaromatic hydrocarbons (PAHs), and volatile organic compounds (VOCs). PM created from biomass combustion is a pollutant particularly damaging to health. This rigorous study employed a personal sampling device and multi-stage cascade impactor to collect airborne PM (including $PM_{2.5}$) and deposited ash from 20 real-world kitchen microenvironments. A robust analysis of the PM was undertaken using a range of morphological, physical, and chemical techniques, the results of which were then compared to a controlled burn experiment. Results revealed that airborne PM was predominantly carbon (~85%), with the OC/EC ratio varying between 1.17 and 11.5. Particles were primarily spherical nanoparticles (50–100 nm) capable of deep penetration into the human respiratory tract (HRT). This is the first systematic characterisation of biomass cooking emissions in authentic rural kitchen settings, linking particle morphology, chemistry and toxicology at health-relevant scales. Toxic heavy metals like Cr, Pb, Cd, Zn, and Hg were detected in PM, while ash was dominated by crustal elements such as Ca, Mg and P. VOCs comprised benzene derivatives, esters, ethers, ketones, tetramethysilanes (TMS), and nitrogen-, phosphorus- and sulphur-containing compounds. This research showcases a unique collection technique that gathered particles indicative of their potential for penetration and deposition in the HRT. Impact stems from the close link between the physico-chemical properties of particle emissions and their environmental and epidemiological effects. By providing a critical evidence base for exposure modelling, risk assessment and clean cooking interventions, this study delivers internationally significant insights. Our methodological innovation, capturing respirable nanoparticles under real-world conditions, offers a transferable framework for indoor air quality research across low- and middle-income countries. The findings therefore advance both fundamental understanding of combustion-derived nanoparticle behaviour and practical knowledge to inform public health, environmental policy, and the UN Sustainable Development Goals.

Keywords: particulate matter; ash; biomass burning; cooking emission; physico-chemical characterisation

check for updates

Academic Editor: Ling Tim Wong

Received: 18 July 2025
Revised: 27 August 2025
Accepted: 29 August 2025
Published: 2 September 2025

Citation: Indu, G.; Saragur Madanayak, S.N.; Ball, R.J. Physico-Chemical Characterisation of Particulate Matter and Ash from Biomass Combustion in Rural Indian Kitchens. *Air* **2025**, *3*, 23. https://doi.org/10.3390/air3030023

Copyright: © 2025 by the authors. Licensee MDPI, Basel, Switzerland. This article is an open access article distributed under the terms and conditions of the Creative Commons Attribution (CC BY) license (https://creativecommons.org/licenses/by/4.0/).

1. Introduction

Indoor Air Pollution (IAP) significantly impacts human health and welfare. Poor indoor air quality (IAQ) causes severe health impacts to the occupants, with women, young children, and elderly being disproportionally affected as they are likely to spend more time indoors. The most common indoor air pollutants include particulate matter (PM), carbon monoxide (CO), carbon dioxide (CO_2), polyaromatic hydrocarbons (PAHs), and volatile organic compounds (VOCs).

PM is of great significance and has been included in the list of pollutants that should be continuously monitored, based on numerous studies focusing on its detrimental effects on human health [1,2]. PM is distinguished by its potentially hazardous and harmful chemical composition. It can significantly impact human health and general air quality, as well as contribute to climate change. Moreover, the health impacts depend on the PM's diameter, where smaller particles pose a more significant threat due to their ability to transport harmful substances deep into the human respiratory system [3,4]. Additionally, factors such as particle shape, aggregation state, and chemical composition, are also important characteristics. Vardoulakis et al. report that increased PM exposure can lead to oxidative stress and inflammation in the lungs, asthma, acute lower respiratory tract infections, and increased risk of exacerbation in patients with Chronic Obstructive Pulmonary Disease (COPD) [5].

VOCs also contribute to poor IAQ, causing headaches, irritation of eyes, and increased risk of cancer [6,7]. Tancrède et al. linked lung irritation, carcinogenesis, teratogenesis, and mutagenesis to exposure to VOCs [8]; Liu et al. associated VOC exposure with optic nerve, brain, heart and kidney damage [9]; and Mølhave reported neurotoxic effects [10]. Irrespective of the toxicity, when the total VOC concentration exceeds 300 $\mu g/m^3$, WHO recommends implementing strategies to reduce levels as effects are cumulative over time [11].

IAQ in rural areas, specifically in kitchen microenvironments of households with no effective extraction, is of increasing concern [12,13]. The choice of unclean fuels, such as solid biomass, further worsens the situation. The largest portion of the fuel access deficit is seen in India alone, where 505 million people (~38%) lack access to clean cooking fuels [14]. Even when clean fuels are available, the practice of fuel stacking is prevalent. Shupler et al. report that 55% of rural households in India prefer biomass fuels over cleaner fuels, even when available [15]. Therefore, a clear understanding of the composition of biomass and cooking emissions is necessary.

Many studies have assessed the indoor air quality of kitchen spaces, primarily based on respirable suspended particulate matter (RSPM) levels [16–19]. However, limited studies have combined IAP and personal exposure studies with detailed physico-chemical characterisation of emissions from cooking activities, particularly when unclean fuels such as solid biomass are used. This represents an important knowledge gap.

Physico-chemical characterisation of particulate matter from different sources, such as diesel exhaust, forest fires, marine sources, smog, and urban areas, has been reported in earlier studies [20–28]. Techniques including scanning electron microscopy (SEM) with energy dispersive X-ray analysis (EDX), inductively coupled plasma with optical emission spectroscopy (ICP-OES), ion chromatography (IC), and total organic carbon (TOC) analysis, are particularly useful for the determination of chemical and morphological characteristics as they can accommodate very small amounts of sample. These methods effectively identify and quantify elements and chemical substances that pose risks to health.

Building on these approaches, this study employs a sampling methodology for measuring the aerodynamic particle size mass distribution of airborne PM as well as deposited ash samples. This method is suitable for routine usage or replication in future studies. It aims to quantitatively and qualitatively characterise PM and ash from kitchen microenvi-

ronments using SEM, EDX, and Raman spectroscopy, considering the significance of PM characterisation with modern techniques toward understanding the impact of these pollutants. Chemical analyses include identifying and quantifying their volatile composition, trace element levels, and carbon content. By combining personal exposure monitoring with cascade impactor sampling, this study introduces a novel, replicable approach to characterising emissions in rural kitchens. The findings of this study validate the approach adopted for the collection and characterisation of particles from kitchens and establish a protocol that can be replicated for similar studies elsewhere.

2. Materials and Methods

This study provides a comprehensive understanding of the physical and chemical characteristics of particulate matter and ash generated from cooking activities, specifically using solid biomass fuels in rural Indian kitchens. Earlier studies have identified particulate matter as having a significant impact on indoor kitchen spaces [16–19,29,30].

Samples of the real-world $PM_{2.5}$ were collected from kitchens whilst cooking was being undertaken. A typical cooking period lasted anywhere between 30 and 90 min depending on the time of the meal and cooking requirements dictated by the type of food being prepared. The study design, location, sample collection and exposure assessment have been previously described in Indu et al. [31]. Features of the real-world kitchens are provided in Appendix A.1.

A controlled burn of the biomass fuels was also performed under laboratory conditions enabling collection of airborne PM and settled ash. Samples of biomass fuel (firewood) collected from the village were burnt for 30 min, with and without cooking, to collect airborne PM samples from 'cooking with biomass fuels' and from 'biomass fuel burning alone'. The control study used a traditional Indian chula (U-shaped small earthen or clay cookstove) as well as a forced draft improved cookstove for the experiments. Care was taken to conduct the real-world monitoring and control studies on normal days, without peak temperatures, humidity or rainfall, to avoid any discrepancies.

Physico-chemical characterisation of all the samples collected from the field and controlled burn were carried out. The diagram in Figure 1 illustrates the methodology followed in this study. The novelty of our approach lies in the combined use of personal exposure monitoring and a multi-stage cascade impactor, which enabled the collection of airborne PM and deposited ash samples representative of their deposition potential in the human respiratory tract. The physical characterisation included particle size distribution, particle morphology and composition, and Raman spectroscopy. The chemical analysis focused on carbonaceous contents, trace elements, and volatile composition.

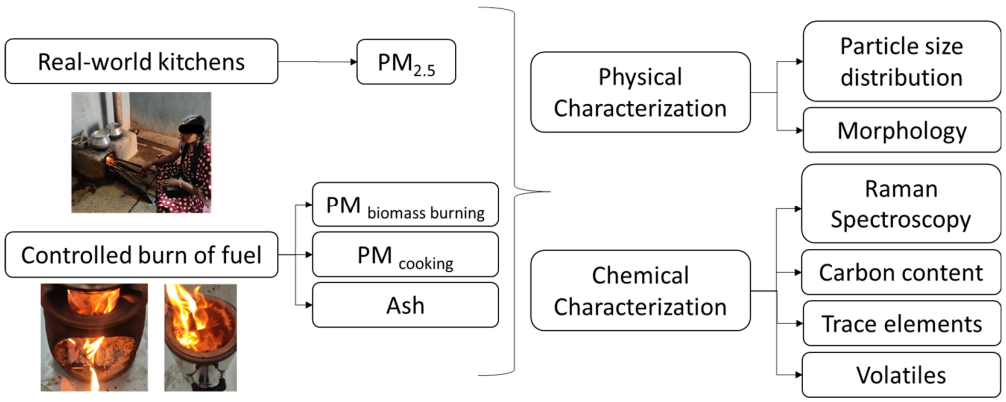


Figure 1. Sample collection under real-world and controlled conditions and the methodologies employed for physical and chemical characterisation.

2.1. Study Area

The real-world samples were collected from 20 kitchen microenvironments from Madahalli village in Mysuru district of Karnataka, India. The village covers an area of 5.6 km^2 with a total population of 1575 people occupying around 365 households [32]. The village was representative of the fuel usage patterns, cooking habits, and socioeconomic status of typical villages in India and was located away from major outdoor pollution sources such as traffic, industry, or construction, thereby minimising external contributions to indoor air quality. The fuel choice of the household was pivotal in the house selection for monitoring, where biomass was the only or primary cooking fuel. The most common kitchen types in the village are separate enclosed kitchens (SK) and open courtyard kitchens (OK), with stove varieties including traditional clay, brick, or concrete cookstoves (TCs) and improved steel or brass natural draft cookstoves (ICs), as seen in Figure 2a,b. Details of kitchen dimensions, kitchen and cookstove configurations, construction materials, and ventilation characteristics (windows, doors, and cross-ventilation) are summarised in Appendix A.1 (Table A1). Controlled burn experiments were conducted under laboratory conditions at the Air Quality Research Laboratory, IIT Madras, Chennai, using the same biomass fuel, collected from the village.



Figure 2. Personal sampling of airborne particulate matter while cooking in real-world kitchens using (**a**) Improved Cookstoves (ICs) and (**b**) Traditional Cookstoves (TCs).

2.2. Instrumentation and Sample Collection

The particulate matter samples were collected from the chosen kitchen locations through personal sampling during cooking periods. The personal PM exposure to the cook was determined through the personal sampling of $PM_{2.5}$. The PM particles were collected through active sampling onto a quartz microfiber filter paper (Whatman Quartz filters circles QM-A size 37 mm, Bangaluru, India). They were placed inside filter cassettes connected to an SKC personal sampler pump (Model PCXR8, SKC Inc., Eighty Four, PA, USA) fitted with an aluminium cyclone. The personal sampling was carried out during the cooking period when the sampler was pinned onto the cook's clothes, as seen in Figure 2a,b, so that the inlet was located within their breathing zone. A flow rate of 2.5 L/min was set to collect the fine PM (<$PM_{2.5}$) on the filter paper in the cassette, and the sample was collected for a cooking period ranging between 30 and 90 min. Background samples for PM and VOCs were collected from the kitchens immediately prior to cooking and were deducted from the cooking-period samples to isolate emissions attributable to cooking activities.

A controlled burn of the biomass fuel from the village was also carried out, and the PM samples from air and ash samples were collected using a cascade impactor. The 6-stage Andersen impactor (Thermo Fisher Scientific, Franklin, MA, USA) mounted with stainless steel collection plates was used [33]. The Andersen impactor utilises a multi-jet cascade impaction apparatus to capture six size-graded aerosol fractions. Each stage contains

400 identical circular holes that the air passes through before being deflected 90° by a stainless-steel collection plate right beneath the jet sieve. As the air flows around the plate to the stage below, particles possessing sufficient inertia are ejected out of the air stream onto the collection plate. Each stage captures smaller particles than the stage before due to greater jet velocities attributed to decreasing jet widths of sequential stages.

The particle size ranges for each of the six stages in the impactor were as follows: Stage 1 (7 µm and above), Stage 2 (4.7 to 7 µm), Stage 3 (3.3 to 4.7 µm), Stage 4 (2.1 to 3.3 µm), Stage 5 (1.1 to 2.1 µm), and Stage 6 (0.65 to 1.1 µm). The sampler's stages represent the human respiratory tract (HRT) [34], as shown in Figure 3. The stages indicate the particle's aerodynamic diameter, which in turn can penetrate the different stages of the HRT. The PM and ash samples were collected on quartz microfiber filter paper (Whatman Quartz filters circles QM-A size 81 mm). The Andersen sampler was operated for the 30-min test period to obtain airborne PM samples, while the settled ash was fed into the sampler inlet and run for 30 min to distribute the ash particles upon filter papers assigned to each size fraction.

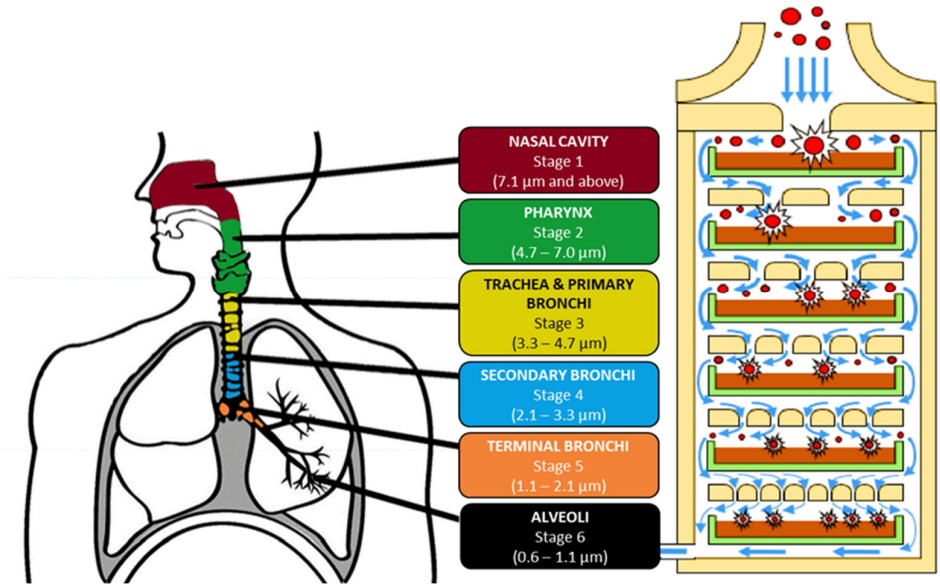


Figure 3. Schematic representation of the 6-stage Andersen sampler and the corresponding stages of the human respiratory tract (HRT) where the particles will penetrate (Part of the figure is adapted from Lindsley et al. [35]).

The PM samples were collected on pre-weighted and conditioned Whatman Quartz filter papers (Whatman, Bangaluru, India) of 37 mm diameter (personal sampling) and 81 mm diameter (controlled burn). The filter papers were baked at 400 °C for 4 h. Following conditioning, they were weighed under controlled temperature and humidity conditions (23 ± 1 °C, 40% RH) for 24 h before and after sampling. The sampled filter papers were stored at −4 °C before further extraction and analysis. The total amounts of PM collected over the periods were measured gravimetrically using a Sartorius ME 5-F microbalance (Sartorius AG, Göttingen, Germany) post-weighing the conditioned filter paper.

The gaseous samples were collected via adsorption using Anasorb coconut shell charcoal (CSC) tubes (SKC Inc., Eighty Four, PA, USA). They were placed inside a sampling head and connected to an SKC personal sampler pump (Model PCXR8, SKC Inc., Eighty Four, PA, USA). The flow rate was set at 0.1–0.2 L/min, and the samples were collected for further chemical analyses. Gaseous samples collected were then sealed and covered with aluminium foils after sampling and stored at −4 °C before further extraction and analysis.

2.3. Physical Characterisation

The particulate matter samples were collected from the chosen kitchen locations through personal sampling during cooking periods to understand their detailed morphology and composition. A controlled burn of the biomass fuel from the village was also carried out in the laboratory, and the PM samples from air and ash samples were collected using a cascade impactor.

2.3.1. Particle Size Distribution

Particle size is an important factor determining the harm that particulate matter can cause to human health. Those less than 10 micrometres are considered most problematic due to their ability to enter the human respiratory tract (HRT) and, in some cases, even the bloodstream. Larger particles can cause irritation to the throat, nose, and eyes. Therefore, the size distribution of particulate matter and ash is important in defining the likely interactions with the human body. Particulate matter is commonly classified into three types, namely ultrafine (aerodynamic diameter less than 1 μm), fine (aerodynamic diameter between 1 and 2.5 μm), and coarse (aerodynamic diameter between 2.5 and 10 μm). Thus, PM_{10}, $PM_{2.5}$, and PM_1 levels are generally considered for particle concentrations and size distributions.

2.3.2. Characterisation Using Field Emission Scanning Electron Microscopy with Energy Dispersive X-Ray Analysis (FE-SEM, EDX)

Both clusters and individual particles deposited on the microfibre filter can be detected using electron microscopy. Samples were analysed using a JEOL JSM-7900F (JEOL Ltd., Akishima, Tokyo, Japan) field emission scanning electron microscope (FE-SEM) fitted with an Aztec Live Ultim Extreme 100 mm^2 (Oxford Instruments, Abingdon, Oxfordshire, UK) low accelerating voltage detector energy dispersive X-ray analysis (EDX). FE-SEM combined with EDX gives information about surface morphology, size, and chemical composition. For SEM sample preparation, sections of 5 mm × 5 mm were cut from the filter papers and mounted with conductive carbon double-sided tape on an aluminium SEM stub for analysis. A Quorum Q150VS Plus Chromium coater (Quorum Technologies Ltd., Laughton, East Sussex, UK) was used to deposit a thin layer of chromium (Cr) to the surface of each sample to improve the conductivity and reduce surface charging. Blank filter analyses confirmed no detectable contamination above background, and only signals above this baseline were reported. Images were obtained at magnifications between 500 and 100,000×. Elemental composition was determined by the integrated energy dispersive X-ray detector (EDX).

2.4. Chemical Characterisation

The samples collected were analysed to determine their chemical composition and constituent elements. Since the samples contain the combustion products of biomass (firewood), their major constituents were expected to contain carbon, followed by trace elements and a wide range of polyaromatic hydrocarbons (PAHs) and volatile organic compounds (VOCs). The samples were extracted using the procedures described prior to analysis.

2.4.1. Raman Spectroscopy

Raman spectroscopy is a spectroscopic technique used to determine the vibrational modes of molecules, which can be used to identify the composition of materials. It is based on the inelastic scattering of monochromatic light, also known as Raman scattering, often from a laser operating in the visible, near-infrared, or near-ultraviolet spectrum [36,37]. The energy of the emitted photons increases or decreases as a result of the laser light's

interactions with phonons, molecular vibrations, or other excitations in the system. The energy shift reveals details about the system's vibrational modes. Raman spectroscopy was carried out for both the ash and PM samples collected using cascade impactors from the controlled burn using a Renishaw inVia confocal Raman microscope (Renishaw, Wotton-under-Edge, Gloucestershire, UK). The characterisations were carried out using a red laser of wavelength 785 nm, 1200-line grating, and a CDD detector.

According to Xu et al., there are two main zones in the range of 800 to 3600 cm^{-1} for organic matter [37]. The first-order Raman spectrum region (FO-RSR) is between 800 and 1800 cm^{-1}, while the second-order Raman spectrum region (SO-RSR) is between 2100 and 3400 cm^{-1}. The regions between 1520 and 1600 cm^{-1} and 1320 and 1360 cm^{-1} are defined as G and D bands, respectively. The appearance of G and D bands in the Raman spectrum is indicative of the presence of amorphous carbon, which is free reactive carbon with no crystalline structure [38,39].

2.4.2. Carbonaceous Analysis

Organic carbon (OC) and Elemental Carbon (EC) were analysed using a DRI Multi-wavelength Thermal/Optical Carbon Analyzer (DRI Model 2015, Multi-wavelength Carbon Analyzer, Magee Scientific, Berkeley, CA, USA). A punch area of 0.5 cm^2 of each quartz filter paper was used for EC/OC analysis for four OC fractions and three EC fractions, following the IMPROVE_A protocol. Blank filter punches were analysed, and all reported OC/EC values exceeded method detection limits for the instrument. It is a thermal protocol used in carbon analysers to quantify carbon fractions evolved at different temperature plateaus and atmospheres [40]. It is derived from the Interagency Monitoring of Protected Visual Environments (IMPROVE) thermal protocol initiated in 1987 [41,42] and is based on the preferential oxidation of OC and EC at different temperatures. OC can be volatilised in a non-oxidising Helium (He) atmosphere, but EC requires combustion by an oxidiser. Further, these volatilised compounds are converted to carbon dioxide (CO_2) by passing them through an oxidiser (heated manganese dioxide, MnO_2). Finally, the CO_2 produced is quantified using a nondispersive infrared (NDIR) CO_2 detector [43,44].

Organic Carbon (OC) refers to the carbon evolved from filter punch in a pure Helium (99.999%) atmosphere at 140, 280, 480, and 580 °C plus pyrolysed organic carbon at each laser wavelength (405, 445, 532, 635, 780, 808, 980) for reflectance (R) and transmittance (T). Elemental Carbon (EC) refers to the carbon evolved from a filter punch in a 98% He/2% O_2 atmosphere at 580, 740, and 840 °C minus any pyrolysed OC at each laser wavelength (405, 445, 532, 635, 780, 808, 980) for reflectance (R) and transmittance (T). OP refers to the carbon evolved from the time that the carrier gas flow is changed from He to 98% He/2% O_2 at 580 °C to the time that the laser-measured filter reflectance (OPR) or transmittance (OPT) reaches its initial value. A negative sign is assigned if the laser split occurs before introducing O_2. Total Carbon (TC) refers to all carbon evolved from the filter punch between ambient and 840 °C under He and 98% He/2% O_2 atmospheres. The carbon analyser can effectively measure between 0.1 and 4000 μg carbon/cm^2 for a typical punch size of 0.5 cm^2.

2.4.3. Elemental Analysis

To analyse the elemental composition, the filter is digested as per USEPA standard operating procedure compendium io-3.1 [45]. A hot-plate digestion method was used to extract metals from the quartz filter paper. The quarter section of the filter was cut into several small fragments and kept in a digestion vessel of 100 mL capacity. An extraction solution was prepared by dissolving 55.5 mL of HNO_3 and 167.5 mL of HCl (1:3 solution). 10 mL of this extraction solution was poured into the digestion vessel and placed over a

hot plate (100 ± 5 °C) for 30 min. Following reflux, the sample was allowed to cool to room temperature. After rinsing the beaker wall with deionised water, 30 mL of reagent water was added, thereby allowing acid from the filter to diffuse out over a period of 30 min. The extracted fluid was filtered using a Millex-GV 0.22 mm syringe filter (Millipore, Bangaluru, India) and transferred to a graduated 50 mL polypropylene centrifuge bottle. Blank filters were also digested in the same way as the sample filters. The extracted sample was then injected into an Optima 5300-DV ICP-OES (Inductively Coupled Plasma with Optical Emission Spectroscopy) (PerkinElmer, Inc., Shelton, CA, USA) to identify the metallic elements viz. silver (Ag), aluminium (Al), arsenic (As), barium (Ba), calcium (Ca), cadmium (Cd), cobalt (Co), chromium (Cr), copper (Cu), iron (Fe), gallium (Ga), mercury (Hg), indium (In), lanthanum (La), magnesium (Mg), manganese (Mn), molybdenum (Mo), nickel (Ni), phosphorous (P), lead (Pb), palladium (Pd), selenium (Se), tin (Sn), zinc (Zn) and zirconium (Zr). The analysis was carried out per USEPA standard operating procedure compendium io-3.5 [46]. Blank quartz filters were digested in parallel and subtracted from sample values; only concentrations above the instrument detection limit were reported.

2.4.4. Analysis of Volatile Organic Compounds (VOCs)

The cooking emissions are a well-known cocktail of multiple volatile chemical compounds, which can be broadly categorised as particle-bound polyaromatic hydrocarbons (PAHs) and gaseous volatile organic compounds (VOCs). Particle-bound PAHs are chemical molecules formed during combustion that have been shown to be genotoxic, carcinogenic, and mutagenic and may have significant negative impacts on the environment and public health. On the other hand, VOC gases are compounds where one of the elements is carbon, with high vapor pressure and low water solubility. They are not all inherently toxic but may cause long-term health effects and can act as irritants or nuisance compounds.

Polycyclic Aromatic Hydrocarbons (PAHs) are a class of organic pollutants containing two or more fused aromatic rings. Incomplete combustion is the primary cause of the majority of PAHs. Due to high selectivity and sensitivity, Gas Chromatography (GC) coupled with Mass Spectrometry (MS) is a powerful instrument for the detection and trace analysis of PAHs. A liquid–liquid extraction method using non-polar solvents such as hexane, dichloromethane and acetone was considered for both particle-bound and gaseous phase samples [47]. Soxhlet extraction was used for the PM samples collected on filter papers, while the volatile and gaseous samples were collected from the adsorbed charcoal medium via ultrasonic extraction.

The collected filter paper samples were covered with aluminium foil and refrigerated at −4 °C until analysis. The ultrasonic-assisted extraction method was followed to isolate the $PM_{2.5}$ collected on filter papers [48]. A quarter of the sampled filter paper was extracted using 50 mL of GC-grade methanol (99.8%) using an ultrasonic bath for 30 min. The extracted sample was filtered with Whatman filter paper no. 41 and then concentrated using a rotary evaporator to a final volume of 2 mL. The sample was then passed through a silica gel column (preconditioned, 60–80 mesh) to remove the impurities. The extract was further concentrated using a rotary evaporator to near dryness under a nitrogen atmosphere. The dried sample was then re-dissolved in 1 mL of methanol and transferred into 2 mL vials for final analysis.

Similarly, the volatile organic compounds (VOCs) present in the gaseous phase, collected using an adsorption medium, such as charcoal, can be extracted and analysed using GC-MS. The samples collected and stored at −4 °C required extraction using GC-grade methanol (99.8%). The Anasorb CSC tube was broken, and the medium was then transferred to a vial containing 10 mL of methanol and sonicated for 10 min. The desorbed sample was then filtered and transferred into 2 mL vials for final analysis. Blank adsorption

tubes were also processed, and analytes were reported only when concentrations exceeded method detection limits.

A Shimadzu single quadrupole GCMS-QP2020 NX gas chromatograph-mass spectrometer (GC-MS) (Shimadzu Corporation, Kyoto, Japan) equipped with SH-I-5Sil MS; non-polar capillary column (30 m × 0.25 mm × 0.25 μm) was used for the particle-bound volatile PAH analysis. 1.5 μL of the sample was injected in split injection mode. The initial temperature for the particle-bound PAH program was 40 °C and held for 1 min. It was then ramped at 20 °C/min to 120 °C and then again to 300 °C at 4 °C/min before being held for 3 min under a helium carrier gas at a constant 2 mL/min flow rate. The solvent delay was set to 0.25 min. The detector was set to scan the analytes using the NIST library, covering specific mass spectra (m/z) ranging from 50 to 800. The mass spectrometer ion source and interface temperatures were 230 °C and 310 °C, respectively, and an analysis time of 55.5 min per sample was used.

For gaseous phase VOC analysis, the GC-MS was equipped with Rtx-VMS; non-polar capillary column (30 m × 0.25 mm × 1.40 μm). 1.5 μL of the sample was injected in split injection mode. The initial temperature for the gaseous phase VOC program was 35 °C and held for 5 min. It was then ramped at 4 °C/min to 60 °C and then again to 225 °C at 8 °C/min and held for 1 min. A helium carrier gas with a constant 1.5 mL/min flow rate and the solvent delay was set to 0.5 min. The detector was set to scan the analytes using the NIST library, covering specific mass spectra (m/z) ranging from 35 to 500. The mass spectrometer ion source and interface temperatures were 220 °C, and the analysis time was 35.5 min per sample.

The temperature programs for both particle-bound and gaseous phase VOC analyses were developed using the Restek Pro EZGC Chromatogram Modeler (Restek Corporation, Bellefonte, PA, USA), which enables modelling of the GC column operation parameters and temperature ramps optimised to the selected compounds and GC columns available. The modelling was performed for the 16 USEPA priority pollutants, namely, naphthalene, acenaphthene, acenaphthylene, fluorene, phenanthrene, anthracene, fluoranthene, pyrene, benzo(a)anthracene, chrysene, benzo(a)pyrene, benzo(b)fluoranthene, benzo(k)fluoranthene, dibenzo(a, h)anthracene, benzo(g, h, i)perylene, and indeno(1,2,3-cd)pyrene [49]. The programs were optimised so that both the highly volatile compounds in the gaseous phase and less volatile compounds in the particle-bound phase could separate efficiently therefore increasing the ability for detection and identification.

3. Results

3.1. Physical Characteristics of Particulate Matter and Ash

3.1.1. Particles Size Distribution

A controlled fuel burn was carried out to collect PM, ash, and gaseous samples. The control sampling used a 6-stage Andersen sampler to understand the size distribution of airborne and settled ash particles in relation to the human respiratory tract. The particle size distributions for PM and ash shown in Figure 4a,b are averaged from triplicate burns, with replicate variation within ±10%. The highest fraction of particles for ash arose from the coarse region (>10 μm). In contrast, cooking produced the highest fraction in the fine region (10–2.5 μm), and biomass burning alone showed the highest fraction in the ultrafine region (<1 μm). The PM mass size distribution for cooking emissions shows a dual peak in the fine and ultrafine regions, indicating the presence of smaller-sized particles that can penetrate deep into the respiratory tract, including the pulmonary region.

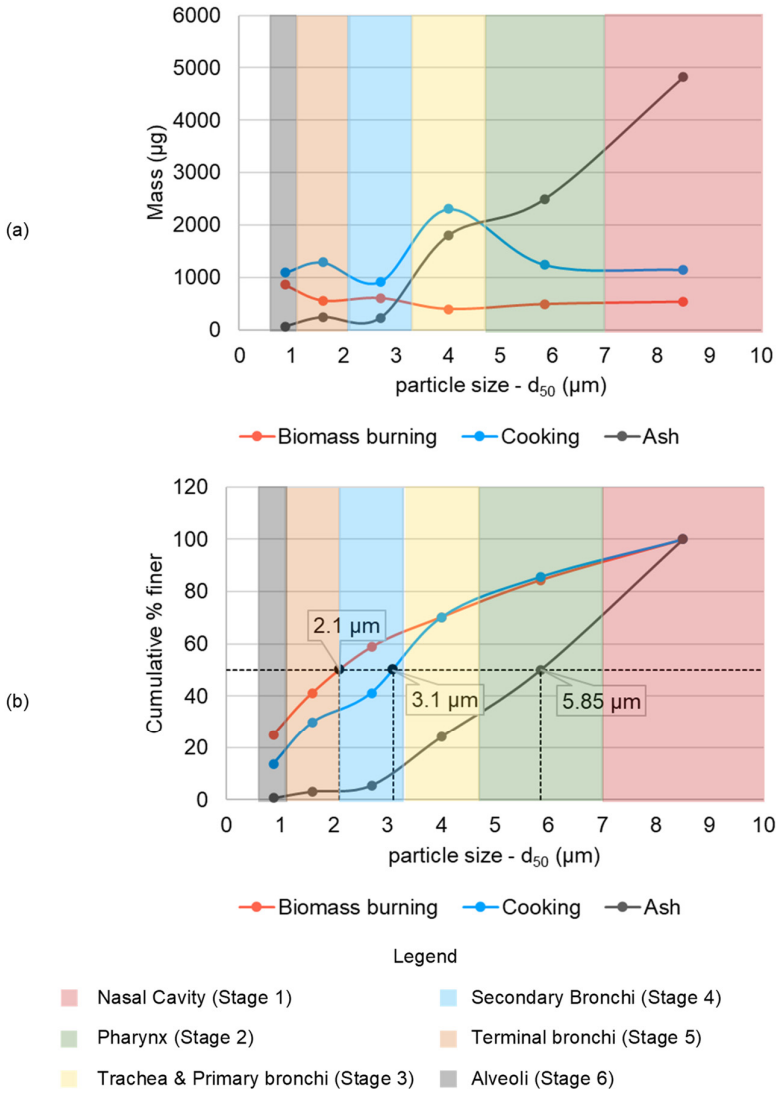


Figure 4. (**a**) Stage-wise mass collected during the controlled burn and (**b**) particle size distribution from the controlled burn (coloured bands representing the 6 stages of HRT).

Similarly, the particle size distribution for the controlled burns in Figure 4b gives the median size of particles for each case, which represents the particle size at which 50% of the sample's particles are smaller and 50% are larger. These suggest that the particles from ash, with a median size of 5.85 µm (coarse particles of size between 10 µm and 2.5 µm), can penetrate only till the head region of the HRT (nasal cavity and pharynx), whereas particles from fuel burning and cooking, with median sizes 2.1 µm and 3.1 µm (fine particles of size between 3.3 µm and 1.1 µm) can penetrate deeper into the tracheobronchial region of HRT (refer Figure 4a,b). The comparison between biomass burning alone and cooking highlights the additional influence of cooking processes (such as heating oil and food ingredients) on particle agglomeration, resulting in differences in particle size distribution. While biomass burning alone produced a higher fraction of ultrafine particles (<1 µm), cooking with biomass fuels showed a greater proportion of fine particles (1–2.5 µm). This shift can be attributed to the influence of cooking processes, promoting agglomeration of smaller particles into larger clusters, altering the effective particle size distribution.

3.1.2. Particle Morphology

The FE-SEM-EDX analysis was used to investigate the samples collected for individual particles' size, shape, surface morphology, and elemental content. Although the difference

between a used and a clean filter paper may be seen with the naked eye, the microscopy methodology provides a clearer understanding of the particulate matter or ash particles deposited on the quartz filters. The FE-SEM images from the kitchen samples of $PM_{2.5}$ showed the presence of large numbers of ultra-fine particles grouped in porous clusters (Figure 5a) as well as soot-like formations with branches or chain-like structures (Figure 5b). This characteristic of the majority of PM consisting of small porous aggregates of micro-crystals is frequently discussed in the literature [20,24,50]. It is most likely the result of the aggregation of smaller particles due to favourable environmental conditions. Further, the EDX results showed that the particles from real-world kitchen samples were predominantly carbon, along with traces of sodium. Contrarily, the ash samples showed C, Ca, Mg, K, Na, P, S, Cl, & Al presence (Table 1). Higher levels of O and Si can be owed to the filter fibres.

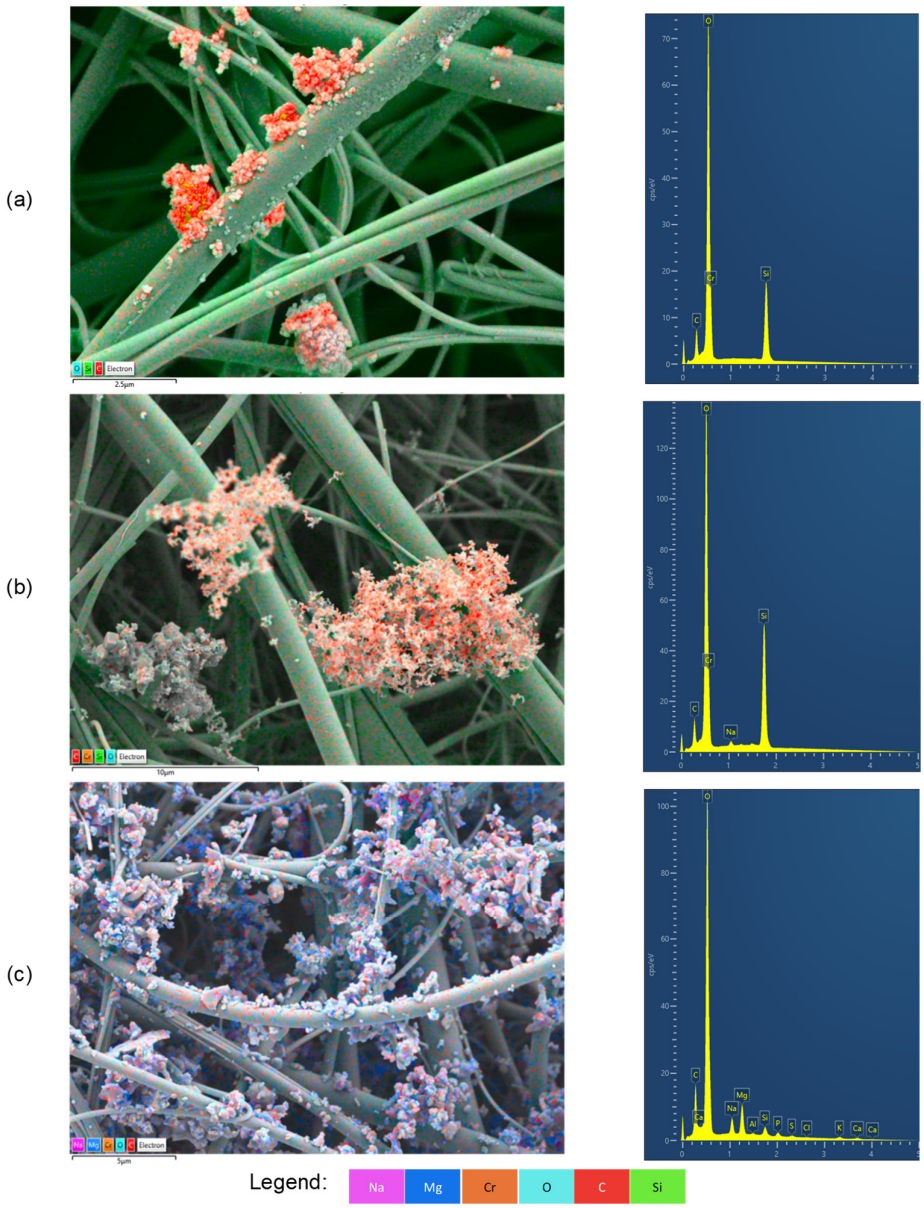


Figure 5. Field emission-scanning electron microscopy (SEM) and corresponding energy dispersive X-ray (EDX) spectra for particles deposited on the filter fibres. *x*-axis range 0 to 5 keV, *y*-axis is intensity in counts per second (cps) eV. (**a**) PM particles agglomerated together, (**b**) PM as soot forming chain-like structures, (**c**) ash particles agglomerated together.

Table 1. Elemental composition of particulate matter (PM) and ash from the energy dispersive X-ray (EDX) results.

Element	Weight %	
	PM	**Ash**
C	6.62	8.50
O	44.08	51.22
Na	0.98	2.03
Mg	-	3.35
Si	48.32	20.42
P	-	1.26
S	-	0.96
Cl	-	0.61
K	-	4.19
Ca	-	6.33
Br	-	1.13
Total:	100	100

From the controlled burn of the biomass fuel, we collected particles at six different stages representative of penetration into the human respiratory system. PM concentration was higher for stages 3 and 4, signifying a greater contribution to PM from sizes ranging between 2.1 and 4.7 μm, similar to the real-time PM sampling observations. As in Figure 6, the PM samples at higher magnifications show that the particles in stages 5 and 6 (smaller sizes) were generally spherical with 50–100 nm diameters. Material captured in stages 3 and 4 are larger agglomerates of smaller particles. As size increases further, in stages 1 and 2, the particles start to lose their spherical shape and agglomerate into flakes or clumps. Morphological features of PM from cooking and biomass burning were broadly similar, with both dominated by spherical ultrafine particles forming aggregates, and no distinct differences that would enable clear source apportionment were observed. The ash samples from the controlled burn (Figure 7) showed higher contributions from stages 5 and 6, contrary to the PM samples, but in agreement with the particle size distribution. The ash particles were of significantly larger sizes (>1 μm) and irregularly shaped. The images from stages 3 and 4 show the clustering of smaller particles to form larger irregularly shaped agglomerates. Stages 1 and 2 show particles significantly larger in size clumped onto the filter fibres, forming large clusters of ash particles. The ash particle morphology was rather hard and irregularly shaped with flaky outgrowths, irregular stacked structures, and a scaly appearance.

3.2. Chemical Characteristics of Particulate Matter and Ash

3.2.1. Carbon Raman Spectrum

The spectra of both the ash and PM samples (Figure 8), from real-world as well as control burn, clearly showed a D-band in the range 1320 to 1360 cm^{-1} and a G-band in the range 1500 to 1600 cm^{-1}, which are characteristic of amorphous carbon [38]. These findings agree with the results from FESEM-EDX, which also confirmed the presence of carbon. The D-to-G peak intensity ration (I_D/I_G) is a commonly used indicator of the degree of structural order in carbonaceous materials [51]. A higher ratio (>1) generally reflects a greater density of defects or a more distorted or amorphous structure, corresponding to a lower degree of graphitization. For the PM and ash samples, the I_D/I_G ratios, calculated from the integrated peak areas, were 1.3 and 1.46, respectively. These values again indicate the predominance of defect-rich, amorphous carbon, consistent with incomplete combustion.

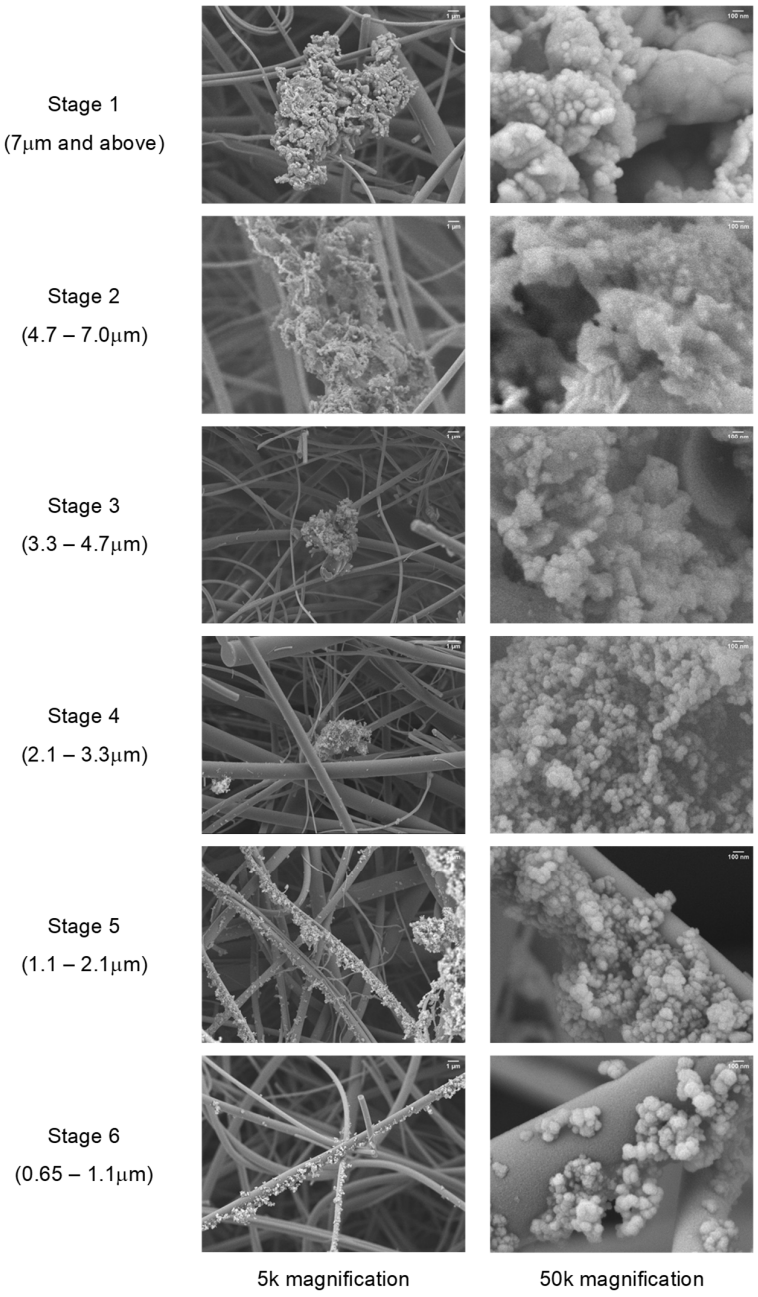


Figure 6. Scanning electron microscopy (SEM) images of PM from the controlled burn of biomass fuel through stages 1 to 6 at magnifications 5000 and 50,000 times.

3.2.2. Carbon Content of PM and Ash from Biomass Combustion

Carbonaceous aerosols comprise two components, i.e., Organic Carbon (OC) and Elemental Carbon (EC). OC can be directly emitted from various sources or atmospheric reactions involving gaseous organic precursors. OC, which makes up the maximum fraction of the carbonaceous aerosol, may either be directly discharged into the environment in particulate form or condense during the conversion of volatile anthropogenic and biogenic reactive organic gases into particles. A wide range of organic compounds are classified as OC. Direct emissions of EC, also known as black carbon (BC) or soot, occur when carbonaceous fuels are burned. Elemental carbon (EC) or black carbon (BC) is only formed when fossil and biomass fuels burn partially, making it a suitable tracer for combustion.

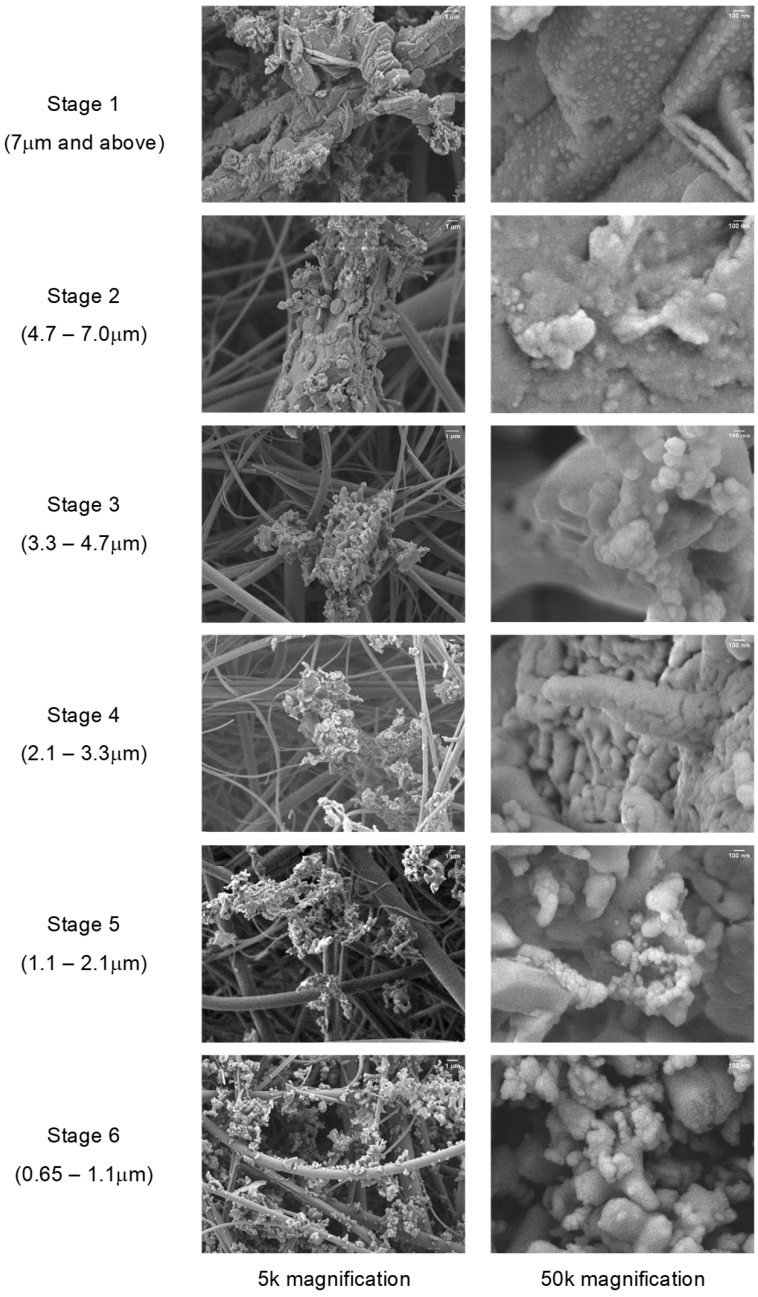


Figure 7. Scanning electron microscopy (SEM) images of ash from the controlled burn of biomass fuel through stages 1 to 6 at magnifications 5000 and 50,000 times.

The $PM_{2.5}$ samples from the real-world kitchens showed carbon content levels between 150 and 250 $\mu g/m^3$. The OC/EC fraction varied between 1.17 and 11.5, which is typical for cooking with biomass fuels. The ratio depends on multiple factors such as the fuel used, stove type, moisture content, and combustion conditions. The average OC/EC ratios for the control study were 6.48, 2.90, and 0.58 for biomass burning, cooking, and ash, respectively. Smouldering has been reported to produce more organic materials with a relatively high OC/EC ratio [52]. This is in agreement with the highest OC/EC ratio observed in $PM_{2.5}$ from biomass burning alone, followed by cooking. Figure 9 shows that 75–87% of the carbon content was OC. Contrarily, only 30% of the ash content was OC, and the remaining 70% was EC, implying an abundance of black carbon or soot from incomplete combustion of solid biomass fuels. This could further point towards adverse health impacts or even chronic health conditions.

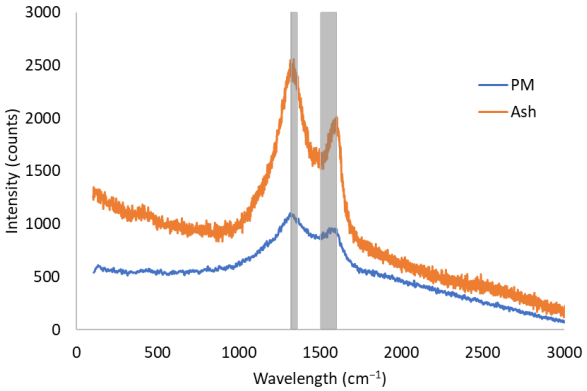


Figure 8. Raman spectra of the particulate matter (PM) and ash samples showing the characteristic D-band and G-band twin peaks of amorphous carbon (shaded regions).

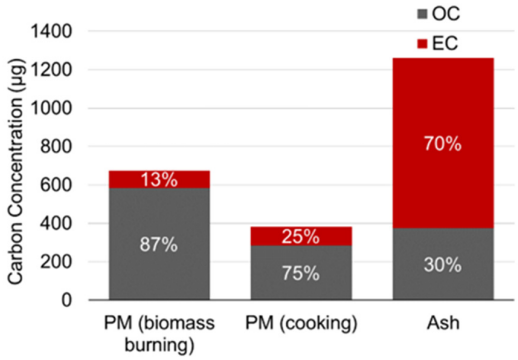


Figure 9. Carbon content of particulate matter (PM) and ash from the controlled burn with their elemental carbon (EC)-organic carbon (OC) composition.

3.2.3. Elemental Composition of Particulate Matter (PM) and Ash from Biomass Combustion

ICP-OES (Inductively coupled plasma-optical emission spectrometry) was used to quantify the composition of elements in the samples. From the elemental analysis carried out (Table 2), the ash composition was predominantly of crustal elements such as calcium (Ca), magnesium (Mg), phosphorous (P), iron (Fe), and aluminium (Al), which are in good agreement with previous studies [53]. PM from biomass burning alone showed higher levels of toxic heavy metals, including arsenic (As), cadmium (Cd), chromium (Cr), lead (Pb), and zinc (Zn). Mercury (Hg) was found only in PM samples from cooking, indicating that the source is the cooking process and not biomass fuels used. Also, the absence of heavy metals like As, Cd, Hg, and Pd in the ash samples is a point of concern, as it implies that heavy metals are present in the airborne PM, which can be inhaled by the occupant, causing adverse health effects. The metal concentrations of As, Cr, Cu, Fe, Ni and Pb from cooking emissions in kitchens were 5.4, 4.0, 2.0, 109.0, 1.2, and 2.4 µg/m^3, respectively, well exceeding the guideline values for ambient air during winter (0.035, 0.026, 0.354, 0.2, 4.3, 0.067 and 0.5 µg/m^3) as set by the WHO air quality guidelines and USEPA regulatory guidelines [54].

The uncontrolled discharge of heavy metals, especially Cr, Pb, Cd, Zn, and Hg, will cause severe damage to the environment and human health. Burning biomass involves numerous intricate physical and chemical processes. When burning biomass, heavy metals may become volatile (Hg), semi-volatile (Cd, Pb, Se), or finitely volatile (Sb, As, Be, Cr, Co, Mn, Ni). In contrast to some minimally volatile metals that remain in the ash, metal condenses on the surface of the solid burning residue particles (fly ash) and is always

present in the exhaust. The burning procedure linked with the properties of the biomass, and the combustion technology affects the emissions.

Table 2. Elemental composition of particulate matter (PM) and ash samples from the controlled burn, determined by inductively coupled plasma optical emission spectroscopy.

Elemental Concentration (µg)	PM (Biomass Burning)	PM (Cooking)	Ash
Ag	0.35	2.94	0.02
Al	8.54	3.87	1.48
As	0.89	0.41	-
Ba	1.01	0.30	0.36
Ca	59.18	31.47	350.05
Cd	0.02	-	-
Co	0.02	-	0.01
Cr	0.29	0.30	0.02
Cu	0.50	0.15	0.07
Fe	17.66	8.21	2.32
Hg	-	1.28	-
In	0.26	0.17	-
La	0.02	-	0.10
Mg	5.88	2.66	31.50
Mn	1.01	0.14	0.18
Mo	0.18	0.05	0.02
Ni	-	0.09	-
P	11.42	4.01	23.79
Pb	1.08	0.18	-
Pd	0.03	-	-
Se	-	-	0.16
Sn	-	0.57	-
Zn	7.71	2.84	0.34
Zr	0.30	0.03	0.01
Legend			
	Highest	Moderate	Lowest

3.2.4. Volatile Constituents of PM and Ash from Biomass Combustion

Volatile analysis was carried out for both particle-bound and gaseous phase samples to find volatile organic compounds (VOCs) and polyaromatic hydrocarbons (PAHs). The chromatogram from the GC-MS analysis was scanned for peaks against the NIST library, and the top 250 peaks were considered as per the area under the curve. The volatile compounds in the samples were classified as shown in Table 3.

Figure 10 shows the volatile composition of the particle-bound and gaseous-phase emissions from the control burn. Both particle-bound volatiles from PM and ash showed similar compositions, where benzene derivatives were the highest, followed by ketones, esters, and silanes. Similarly, for gaseous phase volatile analysis, samples collected during biomass burning alone and cooking showed similar compositions. Benzene derivatives were found to be higher in the particle-bound state than in the gaseous-phase. Common compounds found in the samples include naphthalene derivatives as well as long-chain and cyclic silanes and siloxanes, which cause chronic health effects in addition to being classed as carcinogenic compounds or developmental toxins.

Table 3. Volatile compounds classification used for analysis.

Compounds	Contents Included
Benzene derivatives	Benzaldehyde, indole, phenyl, benzamides, naphthalene derivatives, quinone.
Esters	Esters (acid derivatives).
Ethers	Ethers such as pentabromodiphenyl ether.
Ketones	Benzene substituted, ketones.
Nitrogenous compounds	N-derivatives.
Phosphorous compounds	Compounds with attached phosphorous.
Sulphurous compounds	Compounds with attached sulphur.
TMS	Tetramethyl silanes and its derivatives.
Others	Amides, amines, inorganic compounds, acetates, acids, alkanes, aldehydes, chlorinated compounds, carbonyl compounds, furans, urea, and metal-organics with molybdenum, and osmium.

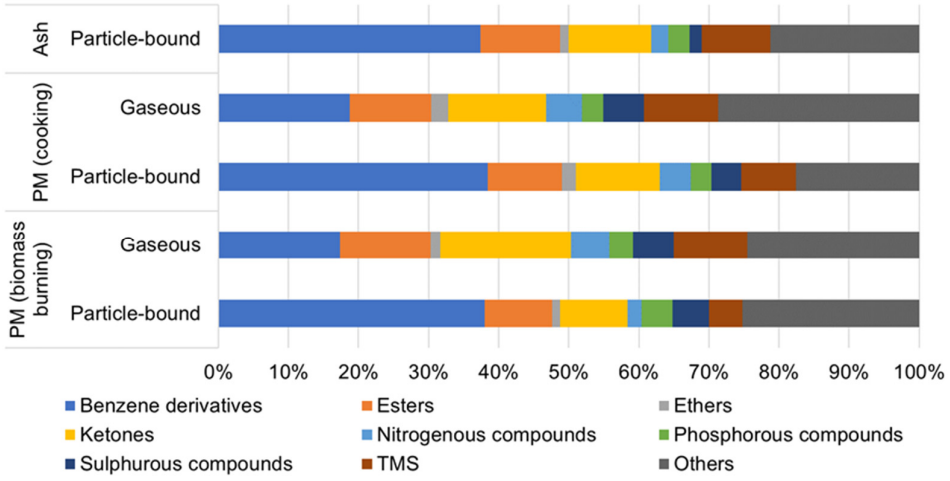


Figure 10. Composition of particle-bound and gaseous-phase volatiles from particulate matter (PM) and ash from the controlled burn.

4. Discussion

The airborne particulate matter is widely recognised as a pollutant of great concern, especially in kitchen microenvironments of developing countries like India, which still rely significantly on solid biomass fuels. A thorough physico-chemical analysis of the PM from biomass combustion while cooking and subsequently generated ash can provide important information relating to composition and, thereby, the risk of exposure. A novel sampling procedure was showcased combining airborne PM, gaseous as well as settled ash collection using active sampling techniques. Importantly, this methodology is representative of the human respiratory tract and therefore reveals how PM can penetrate the HRT. Sophisticated analyses and measurement techniques such as FE-SEM-EDX, Raman spectrometry, TOC analyser, ICP-OES, and GC-MS were employed for the physico-chemical characterisation of the samples. The morphology of the airborne PM revealed the presence of carbonaceous nanoparticles of sizes ~100 nm, which can be potentially hazardous to humans upon entry to the HRT, and subsequently the bloodstream, through alveoli. In addition, the chemical composition of said particles revealed the presence of toxic heavy metals including Cr, Pb, Cd, Zn and Hg, as well as multiple harmful volatile organic compounds. Figure 11 presents a comparative representation of the chemical composition of PM from biomass burning and cooking along with the deposited ash. Carbon (OC + EC) contributed close to 85% of the PM and 60% of the ash composition. This was followed by crustal elements, heavy

metals, and volatile organics. The results obtained were in agreement with similar studies carried out for hazardous PM or ash from combustion sources such as diesel engines, forest fires, etc. [22–25].

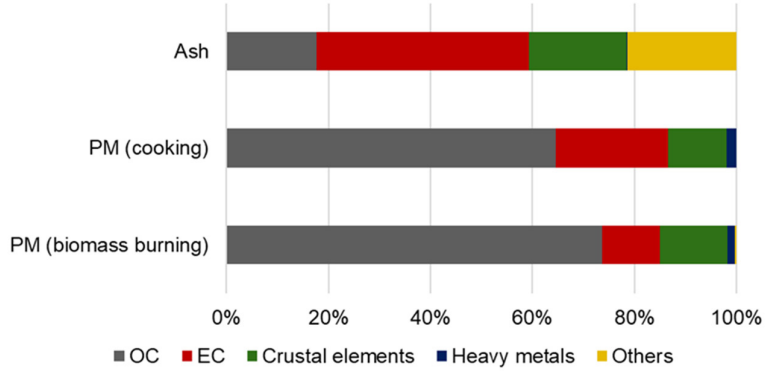


Figure 11. Overall chemical composition of PM and ash from the controlled burn.

The physico-chemical characteristics observed in this study carry clear health and environmental implications. The presence of carbonaceous nanoparticles (50–100 nm) is of particular concern, as such particles can penetrate deeply into the alveolar region of the lungs and even enter the bloodstream, contributing to systemic effects such as cardiovascular disease and neurological impacts [3,5,22]. Although not directly inhaled, ash may contribute to secondary exposures via resuspension or dermal contact, given its content of toxic metals and residual organics. The detection of heavy metals including Cr, Pb, Cd, Zn, and Hg in airborne PM is significant given their well-documented toxicity, with risks ranging from respiratory irritation and oxidative stress to neurotoxicity and carcinogenicity [20,23,25]. Similarly, the wide range of VOCs identified, including benzene derivatives, ketones, and silanes, are linked to acute effects such as airway irritation as well as long-term risks like cancer [6–9]. From an environmental perspective, the high elemental carbon fraction suggests substantial black carbon content, which is a potent short-lived climate forcer contributing to regional warming and poor air quality [24,28].

These findings are consistent with previous studies reporting adverse health and environmental impacts of biomass combustion [16–19,29,30,50], while extending the evidence by combining personal exposure sampling with detailed chemical and morphological analyses. For instance, our detection of mercury specifically in cooking emissions, rather than biomass burning alone, highlights the importance of considering cooking processes themselves as a source of toxic pollutants. By situating our results alongside these earlier studies, the work strengthens the evidence that household biomass combustion is a critical driver of both health burdens and environmental impacts in rural settings.

Although the study involved 20 kitchens within a single village in southern India, this focused design enabled high-resolution characterisation of authentic cooking environments rarely documented in the literature. Controlled burn experiments with firewood, while centred on one biomass type, provided a robust reference dataset against which real-world emissions could be benchmarked, enhancing the reliability of interpretation. While detailed physico-chemical characterisation was prioritised, toxicological and epidemiological linkages were deliberately scoped for future investigation, with the present dataset providing a critical foundation for such work. Similarly, although temporal variations in exposure were not analysed here, real-time $PM_{2.5}$ concentrations were measured and reported in Indu et al. [31], ensuring that the wider exposure context is available. Importantly, the study establishes a replicable and innovative methodology combining personal exposure monitoring with cascade impactor sampling, which can be scaled up to multi-site, multi-season

studies, extended across diverse fuels and stove types, and integrated with health outcome assessments to generate even greater international impact. Future work could also apply enrichment factor (EF) analysis to quantitatively distinguish crustal versus anthropogenic sources of metals and build on this dataset to convert metal concentrations into inhalable burdens and exposure doses, thereby strengthening the link to health risk assessment. Such extensions will strengthen the evidence base on exposure–response relationships and support interventions for clean cooking transitions in rural communities.

5. Conclusions

This study demonstrates a replicable approach that combines personal exposure monitoring with a six-stage Andersen cascade impactor to collect particulate samples representative of their deposition potential in the human respiratory tract, followed by detailed physico-chemical characterisation (FE-SEM-EDX, Raman, carbon fractions, ICP-OES, and GC-MS). Cooking with biomass fuels produced agglomerated carbonaceous nanoparticles (∼50–100 nm) and a high carbon fraction (OC + EC), with the mass size distribution during cooking peaking at d50 ~3 μm, indicative of penetration into the tracheobronchial region, while biomass burning alone yielded a larger proportion of ultrafine particles (<1 μm), consistent with agglomeration during food/oil heating increasing effective particle sizes. Toxic heavy metals (Cr, Pb, Cd, Zn, and Hg) were detected in particulate matter, with mercury attributable to the cooking process rather than the fuel, and a range of volatile organics (including benzene derivatives, ketones, and silanes) were identified. The results provide a unique insight into the detailed qualitative assessment of ash and particulate matter generated during cooking. This is essential to enable environmental and epidemiological investigations related to rural Indian kitchens and solid biomass fuel usage. The findings of this study have important policy and public health implications as well. Targeted interventions such as improved stove design, enhanced kitchen ventilation, and fuel switching to cleaner alternatives can substantially reduce carbonaceous PM emissions and associated toxicity. The detection of toxic heavy metals and hazardous VOCs in biomass cooking emissions highlights the urgency of accelerating access to clean cooking fuels and improved stove technologies in rural India. Policy measures should prioritise subsidies and infrastructure to promote liquefied petroleum gas (LPG), electricity, and renewable energy-based cooking solutions, while discouraging continued reliance on biomass. At the same time, integrating household air quality monitoring into public health programs and conducting awareness campaigns to inform rural communities about the health risks of biomass smoke are critical. Such interventions will not only reduce household air pollution exposure but also contribute to achieving broader climate and sustainable development goals. Additionally, the use of controlled burn experiments, a multi-stage cascade impactor, and unique collection techniques and the identification of pollutants, along with the establishment of a replicable protocol, enhances the study's relevance to public health and its reliability for future research.

Author Contributions: G.I.: Conceptualization, Methodology, Validation, Formal Analysis, Investigation, Writing—original draft preparation, Writing—review and editing, Visualisation. S.N.S.M.: Resources, Writing—review and editing, Supervision, Project Administration, Funding Acquisition. R.J.B.: Resources, Writing—review and editing, Supervision, Project Administration, Funding Acquisition. All authors have read and agreed to the published version of the manuscript.

Funding: Part of the study was supported by the Climate-Resilient Energy Secure and healthy built environmenTs (CREST) project. CREST is supported by a Going Global Partnerships—Collaborative Grant from the British Council's Going Global Partnerships programme [grant number 877766384]. The program builds stronger, more inclusive, internationally connected higher education and TVET (Technical and Vocational Education and Training) systems.

Institutional Review Board Statement: Ethical review and approval were waived for this study as it involved human participation solely for environmental data collection, with no collection of human or biological samples.

Informed Consent Statement: Informed consent was obtained from all participants involved in the study for the monitoring and collection of air samples from their kitchens.

Data Availability Statement: The raw data supporting the conclusions of this article will be made available by the authors on request. All relevant data have been summarized in the article through tables and figures. Specific datasets can be made available upon request by contacting the corresponding author.

Use of Artificial Intelligence: AI-assisted tools were used for grammar correction and language editing in the preparation of this manuscript.

Acknowledgments: The authors thank Philip Fletcher, University of Bath, for his technical input and guidance for Raman spectroscopy, electron imaging and EDX analysis. Support from the Sophisticated Analytical Instruments Facility (SAIF) at IIT Madras for their help with laboratory analyses is also acknowledged. We would also like to thank the people of Madahalli village for providing access to their kitchens to enable monitoring, and Mahesh PA and associates, JSS Medical College and Academy of Higher Education and Research, Mysuru, Karnataka, for supporting the field campaign and study.

Conflicts of Interest: The authors declare that they have no known competing financial interests or personal relationships that could have appeared to influence the work reported in this paper. The funders had no role in the design of the study; in the collection, analyses, or interpretation of data; in the writing of the manuscript; or in the decision to publish the results.

Abbreviations

The following abbreviations are used in this manuscript:

COPD	Chronic Obstructive Pulmonary Disease
CSC	Coconut Shell Charcoal
EC	Elemental Carbon
EDX	Energy Dispersive X-ray Analysis
EF	Enrichment Factor
FE-SEM	Field Emission-Scanning Electron Microscope
FO-RSR	First-Order Raman Spectrum Region
GC-MS	Gas Chromatography-Mass Spectrometry
HRT	Human Respiratory Tract
IAP	Indoor Air Pollution
IAQ	Indoor Air Quality
ICs	Improved Cookstoves
ICP-OES	Inductively Coupled Plasma with Optical Emission Spectroscopy
IMPROVE	Interagency Monitoring of Protected Visual Environments
LPG	Liquefied Petroleum Gas
NDIR	Non-Dispersive Infrared
OC	Organic Carbon
OK	Open Kitchen
PAHs	Polyaromatic Hydrocarbons
PM	Particulate Matter
SK	Separate Kitchen
SO-RSR	Second-Order Raman Spectrum Region
TC	Total Carbon
TCs	Traditional Cookstoves
TMS	Tetramethylsilane
TOC	Total Organic Carbon

VOCs Volatile Organic Compounds

Appendix A

Appendix A.1. Characteristics of Real-World Rural Kitchens

The real-world kitchens were chosen from Madahalli village of Karnataka state, India. The choice of the house mainly depended on the fuel used for cooking, which was solid biomass, such as firewood, agricultural residue and crop residue. The houses were single-story buildings occupied by single or joint families. The average occupancy was 4.7 people. Table summarise the characteristics of the kitchens monitored. 45% of the kitchens studied can be classified as "small" with respect to their volume (less than 30 m^3). Smaller kitchen volume led to the build-up of pollutant concentrations due to reduced pollutant dispersion. Further, 55% of the monitored kitchen locations lacked any window or ventilation system other than a door connecting it to the rest of the house. Only 20% of the kitchens studied satisfied the cross-ventilation requirement with their door and window placements. This further reduces any chance of ventilation and, thus, pollutant removal from the enclosed kitchen locations.

Table A1. Summary of the construction materials and dimensions of the studied real-world kitchens.

House Code	No. of Occupants	Kitchen and Cookstove Configuration *	Construction Materials for the Kitchen	Dimensions of the Kitchen (Length × Breadth × Height) (m)	Volume (m^3)	No. of Windows in the Kitchen	Dimension of Windows (Height × Breadth) (m)	No. of Doors in the Kitchen	Dimension of Doors (Height × Breadth) (m)	Does the Location of Doors/Windows Allow Cross-Ventilation
M01	8	OK_IC	Brick wall, concrete floor and tiled roof	4 × 2 × 3	24	1	1 × 1	1	1 × 2	No
M02	4	OK_TC	Brick wall, concrete floor and tiled roof	5 × 4 × 3	60	0		2	1 × 2	No
M03	4	OK_IC	Brick wall, concrete floor and tiled roof	4 × 4 × 3	48	1	0.5 × 0.75	2	1 × 2	Yes
M04	4	OK_IC	Brick wall, concrete floor and tiled roof	2 × 2 × 2.5	10	0		1	0.8 × 1.8	No
M05	5	SK_TC	Brick wall, concrete floor and tiled roof	10 × 5 × 3	150	4	1 × 1	2	2.5 × 1	No
M06	3	SK_TC	Brick wall, concrete floor and tiled roof	2 × 3 × 3	18	1	1 × 1	1	2.5 × 0.8	No
M07	5	SK_TC	Brick wall, concrete floor and tiled roof	3 × 4 × 3	36	1	1 × 1	2	2.5 × 1	No
M08	5	SK_IC	Brick wall, concrete floor and tiled roof	3 × 4 × 3	36	1	1 × 1	2	2.5 × 1	No
M09	3	SK_TC	Brick wall, concrete floor and tiled roof	6 × 5 × 3	90	2	1.5 × 1	2	2.5 × 1	Yes
M10	3	OK_IC	Brick wall, mud floor and tiled roof	3 × 4 × 3	36	0		1	2 × 1	No
M11	7	OK_TC	Mud wall, mud floor and tiled roof	1.5 × 2 × 2.5	7.5	0		1	2.5 × 1	No
M12	3	SK_TC	Brick wall, mud floor and tiled roof	2 × 2 × 2.5	10	0		1	2.5 × 1	No
M13	5	SK_TC	Brick wall, concrete floor and tiled roof	3 × 2 × 3	18	0		1	2.5 × 1	No
M14	4	SK_TC	Brick wall, concrete floor and tiled roof	1.5 × 1.5 × 2.5	5.625	0		1	2.5 × 1	No
M15	4	OK_TC	Brick wall, concrete floor and tiled roof	2 × 3 × 3	18	0		1	2.5 × 1	No
M16	8	SK_TC	Brick wall, concrete floor and tiled roof	3 × 4 × 3	36	0		2	2.5 × 1	Yes
M17	6	SK_TC	Brick wall, concrete floor and tiled roof	5 × 6 × 3	90	2	0.8 × 0.8	1	1.2 × 2.5	No
M18	6	OK_TC	Brick wall, concrete floor and tiled roof	3 × 2 × 3	18	0		1	2.5 × 1	No
M19	3	SK_IC	Brick wall, concrete floor and tiled roof	2 × 2 × 3	12	0		1	2.5 × 1	No
M20	4	SK_IC	Brick wall, concrete floor and tiled roof	2 × 3.5 × 3	21	1	1 × 1.5	1	2.5 × 0.8	Yes

* SK: Separate Kitchen; OK: Open Kitchen; TC: Traditional Cookstove; IC: Improved Cookstove.

References

1. Bruce, N.; Pope, D.; Rehfuess, E.; Balakrishnan, K.; Adair-Rohani, H.; Dora, C. WHO indoor air quality guidelines on household fuel combustion: Strategy implications of new evidence on interventions and exposure–risk functions. *Atmos. Environ.* **2015**, *106*, 451–457. [CrossRef]
2. WHO. *WHO Guidelines for Indoor Air Quality: Household Fuel Combustion*; WHO Document Production Services: Geneva, Switzerland, 2014; Available online: https://www.who.int/publications/i/item/9789241548885 (accessed on 21 June 2024).
3. Deepthi, Y.; Shiva Nagendra, S.M.; Gummadi, S.N. Characteristics of indoor air pollution and estimation of respiratory dosage under varied fuel-type and kitchen-type in the rural areas of Telangana state in India. *Sci. Total Environ.* **2019**, *650*, 616–625. [CrossRef]
4. Varghese, S.K.; Gangamma, S.; Patil, R.S.; Sethi, V. Particulate Respiratory Dose to Indian Women from Domestic Cooking. *Aerosol Sci. Technol.* **2005**, *39*, 1201–1207. [CrossRef]
5. Vardoulakis, S.; Giagloglou, E.; Steinle, S.; Davis, A.; Sleeuwenhoek, A.; Galea, K.S.; Dixon, K.; Crawford, J.O. Indoor exposure to selected air pollutants in the home environment: A systematic review. *Int. J. Environ. Res. Public Health* **2020**, *17*, 8972. [CrossRef] [PubMed]
6. Zhu, J.; Wong, S.L.; Cakmak, S. Nationally representative levels of selected volatile organic compounds in canadian residential indoor air: Population-based survey. *Environ. Sci. Technol.* **2013**, *47*, 13276–13283. [CrossRef]
7. Jurvelin, J.; Vartiainen, M.; Jantunen, M.; Pasanen, P. Personal exposure levels and microenvironmental concentrations of formaldehyde and acetaldehyde in the Helsinki metropolitan area, Finland. *J. Air Waste Manag. Assoc.* **2001**, *51*, 17–24. [CrossRef]
8. Tancrède, M.; Wilson, R.; Zeise, L.; Crouch, E. The carcinogenic risk of some organic vapors indoors: A theoretical survey. *Atmos. Environ. (1967)* **1987**, *21*, 2187–2205. [CrossRef]
9. Liu, S.; Thompson, S.L.; Stark, H.; Ziemann, P.J.; Jimenez, J.L. Gas-Phase Carboxylic Acids in a University Classroom: Abundance, Variability, and Sources. *Environ. Sci. Technol.* **2017**, *51*, 5454–5463. [CrossRef]
10. Mølhave, L. Indoor climate, air pollution, and human comfort. *J. Expo. Anal. Environ. Epidemiol.* **1991**, *1*, 63–81. Available online: https://pubmed.ncbi.nlm.nih.gov/1824312/ (accessed on 21 June 2024). [PubMed]
11. WHO. WHO Guidelines for Indoor Air Quality: Selected Pollutants. 2010. Available online: https://www.who.int/publications/i/item/9789289002134 (accessed on 21 June 2024).
12. Albadra, D.; Kuchai, N.; Acevedo-De-Los-Ríos, A.; Rondinel-Oviedo, D.; Coley, D.; da Silva, C.; Rana, C.; Mower, K.; Dengel, A.; Maskell, D.; et al. Measurement and analysis of air quality in temporary shelters on three continents. *Build. Environ.* **2020**, *185*, 107259. [CrossRef]
13. Klansek, T.; Coley, D.A.; Paszkiewicz, N.; Albadra, D.; Rota, F.; Ball, R.J. Analysing experiences and issues in self-built shelters in Bangladesh using transdisciplinary approach. *J. Hous. Built Environ.* **2021**, *36*, 723–757. [CrossRef]
14. WHO. Access To Clean Fuels and Technologies for Cooking. In *Tracking SDG 7: The Energy Progress Report 2023*; WHO: Washington, DC, USA, 2023; pp. 66–96. Available online: https://www.who.int/publications/m/item/tracking-sdg7{-}{-}the-energy-progress-report-2023 (accessed on 21 June 2024).
15. Shupler, M.; Hystad, P.; Birch, A.; Miller-Lionberg, D.; Jeronimo, M.; Arku, R.E.; Chu, Y.L.; Mushtaha, M.; Heenan, L.; Rangarajan, S.; et al. Household and personal air pollution exposure measurements from 120 communities in eight countries: Results from the PURE-AIR study. *Lancet Planet. Health* **2020**, *4*, e451–e462. [CrossRef] [PubMed]
16. Lachowicz, J.I.; Milia, S.; Jaremko, M.; Oddone, E.; Cannizzaro, E.; Cirrincione, L.; Malta, G.; Campagna, M.; Lecca, L.I. Cooking Particulate Matter: A Systematic Review on Nanoparticle Exposure in the Indoor Cooking Environment. *Atmosphere* **2023**, *14*, 12. [CrossRef]
17. Ansari, F.A.; Khan, A.H.; Patel, D.K.; Siddiqui, H.; Sharma, S.; Ashquin, M.; Ahmad, I. Indoor exposure to respirable particulate matter and particulate-phase PAHs in rural homes in North India. *Environ. Monit. Assess.* **2009**, *170*, 491–497. [CrossRef]
18. Abdullahi, K.L.; Delgado-Saborit, J.M.; Harrison, R.M. Emissions and indoor concentrations of particulate matter and its specific chemical components from cooking: A review. *Atmos. Environ.* **2013**, *71*, 260–294. [CrossRef]
19. Balakrishnan, K.; Sankar, S.; Parikh, J.; Padmavathi, R.; Srividya, K.; Venugopal, V.; Prasad, S.; Pandey, V.L. Daily average exposures to respirable particulate matter from combustion of biomass fuels in rural households of southern India. *Environ. Health Perspect.* **2002**, *110*, 1069–1075. [CrossRef]
20. Bodor, M.; Ceoromila, A.; Başliu, V. Morphological and Chemical Characterization of Particulate Matter from an Indoor Measuring Campaign. *Sustainability* **2022**, *14*, 11621. [CrossRef]
21. Budhavant, K.B.; Gawhane, R.D.; Rao, P.S.P.; Nair, H.R.C.R.; Safai, P.D. Physico-chemical characterization and sink mechanism of atmospheric aerosols over South-west India. *J. Atmos. Chem.* **2020**, *77*, 17–33. [CrossRef]
22. Fatima, S.; Mishra, S.K.; Ahlawat, A.; Dimri, A.P. Physico-Chemical Properties and Deposition Potential of $PM_{2.5}$ during Severe Smog Event in Delhi, India. *Int. J. Environ. Res. Public Health* **2022**, *19*, 15387. [CrossRef] [PubMed]

23. Karin, P.; Koko, P.; Charoenphonphanich, C.; Chollacoop, N.; Hanamura, K. Physicochemical Characterization of Diesel Engine's Soot and Metal Oxide Ash Nanoparticles Using Electron Microscopy, EDS and TGA. *Emiss. Control. Sci. Technol.* **2021**, *7*, 91–104. [CrossRef]
24. Oo, H.M.; Karin, P.; Chollacoop, N.; Hanamura, K. Physicochemical characterization of forest and sugarcane leaf combustion's particulate matters using electron microscopy, EDS, XRD and TGA. *J. Environ. Sci.* **2021**, *99*, 296–310. [CrossRef] [PubMed]
25. Zeraati-Rezaei, S.; Alam, M.S.; Xu, H.; Beddows, D.C.; Harrison, R.M. Size-resolved physico-chemical characterization of diesel exhaust particles and efficiency of exhaust aftertreatment. *Atmos. Environ.* **2020**, *222*, 117021. [CrossRef]
26. Fanizza, C.; De Berardis, B.; Ietto, F.; Soggiu, M.E.; Schirò, R.; Inglessis, M.; Ferdinandi, M.; Incoronato, F. Analysis of major pollutants and physico-chemical characteristics of PM2.5 at an urban site in Rome. *Sci. Total Environ.* **2018**, *616–617*, 1457–1468. [CrossRef]
27. Cachon, F.B.; Cazier, F.; Verdin, A.; Dewaele, D.; Genevray, P.; Delbende, A.; Ayi-Fanou, L.; Aïssi, F.; Sanni, A.; Courcot, D. Physicochemical Characterization of Air Pollution Particulate Matter ($PM_{2.5}$ and $PM_{>2.5}$) in an Urban Area of Cotonou, Benin. *Atmosphere* **2023**, *14*, 201. [CrossRef]
28. Parent, P.; Laffon, C.; Trillaud, V.; Grauby, O.; Ferry, D.; Limoges, A.; Missamou, T.; Piazzola, J. Physicochemical Characterization of Aerosols in the Coastal Zone: Evidence of Persistent Carbon Soot in the Marine Atmospheric Boundary Layer (MABL) Background. *Atmosphere* **2023**, *14*, 291. [CrossRef]
29. Gogoi, D.; Sazid, A.; Bora, J.; Deka, P.; Balachandran, S.; Hoque, R.R. Particulate matter exposure in biomass-burning homes of different communities of Brahmaputra Valley. *Environ. Monit. Assess.* **2021**, *193*, 856. [CrossRef] [PubMed]
30. Massey, D.D.; Kulshrestha, A.; Taneja, A. Particulate matter concentrations and their related metal toxicity in rural residential environment of semi-arid region of India. *Atmos. Environ.* **2013**, *67*, 278–286. [CrossRef]
31. Indu, G.; Shiva, N.S.; Mahesh, P.A. Indoor air pollution in rural south Indian kitchens from biomass-fuel usage and the predicted lung deposition in women. *Atmos. Environ.* **2024**, *336*, 120732. [CrossRef]
32. Census India, Office of the Registrar General & Census Commissioner, India Ministry of Home Affairs, Government of India. 2011. Available online: https://censusindia.gov.in/census.website/data/population-finder (accessed on 14 February 2021).
33. O'Donnell, H.; Montgomery, T.; Corn, M. Routine assessment of the particle size-weight distribution of urban aerosols. *Atmos. Environ. (1967)* **1970**, *4*, 1–7. [CrossRef]
34. Agarwal, S.; Mandal, P.; Srivastava, A. Quantification and Characterization of Size-segregated Bioaerosols at Municipal Solid Waste Dumping Site in Delhi. *Procedia Environ. Sci.* **2016**, *35*, 400–407. [CrossRef]
35. Lindsley, W.G.; Green, B.J.; Blachere, F.M.; Martin, S.B.; Law, B.F.; Jensen, P.A.; Schafer, M.P. Chapter BA: Sampling and Characterization of Bioaerosols. In *NIOSH Manual of Analytical Methods (NMAM)*, 5th ed.; NIOSH: Washington, DC, USA; pp. BA1–BA115.
36. Liu, Y.; Sun, B.; Tajcmanova, L.; Liu, C.; Wu, J. Effect of carbon residues structures on burnout characteristic by FTIR and Raman spectroscopy. *Spectrochim. Acta Part A Mol. Biomol. Spectrosc.* **2022**, *272*, 120947. [CrossRef]
37. Xu, J.; He, Q.; Xiong, Z.; Yu, Y.; Zhang, S.; Hu, X.; Jiang, L.; Su, S.; Hu, S.; Wang, Y.; et al. Raman spectroscopy as a versatile tool for investigating thermochemical processing of coal, biomass, and wastes: Recent advances and future perspectives. *Energy Fuels* **2020**, *35*, 2870–2913. [CrossRef]
38. Dychalska, A.; Popielarski, P.; Franków, W.; Fabisiak, K.; Paprocki, K.; Szybowicz, M. Study of CVD diamond layers with amorphous carbon admixture by Raman scattering spectroscopy. *Mater. Sci.* **2015**, *33*, 799–805. [CrossRef]
39. Marina-Montes, C.; Pérez-Arribas, L.V.; Anzano, J.; de Vallejuelo, S.F.-O.; Aramendia, J.; Gómez-Nubla, L.; de Diego, A.; Madariaga, J.M.; Cáceres, J.O. Characterization of atmospheric aerosols in the Antarctic region using Raman Spectroscopy and Scanning Electron Microscopy. *Spectrochim. Acta Part A Mol. Biomol. Spectrosc.* **2022**, *266*, 120452. [CrossRef]
40. Watson, J.G.; Chow, J.C.; Chen, L.-W.A. Summary of Organic and Elemental Carbon/Black Carbon Analysis Methods and Intercomparisons. *Aerosol Air Qual. Res.* **2005**, *5*, 65–102. [CrossRef]
41. Chow, J.C.; Watson, J.G.; Chen, L.-W.A.; Paredes-Miranda, G.; Chang, M.-C.O.; Trimble, D.; Fung, K.K.; Zhang, H.; Yu, J.Z. Refining temperature measures in thermal/optical carbon analysis. *Atmos. Chem. Phys.* **2005**, *5*, 2961–2972. [CrossRef]
42. Chow, J.C.; Watson, J.G.; Chen, L.-W.A.; Chang, M.O.; Robinson, N.F.; Trimble, D.; Kohl, S. The IMPROVE_A temperature protocol for thermal/optical carbon analysis: Maintaining consistency with a long-term database. *J. Air Waste Manag. Assoc.* **2007**, *57*, 1014–1023. [CrossRef]
43. Chen, L.-W.A.; Chow, J.C.; Wang, X.L.; Robles, J.A.; Sumlin, B.J.; Lowenthal, D.H.; Zimmermann, R.; Watson, J.G. Multi-wavelength optical measurement to enhance thermal/optical analysis for carbonaceous aerosol. *Atmos. Meas. Tech.* **2015**, *8*, 451–461. [CrossRef]
44. Chow, J.C.; Wang, X.; Sumlin, B.J.; Gronstal, S.B.; Chen, L.-W.A.; Trimble, D.L.; Kohl, S.D.; Mayorga, S.R.; Riggio, G.; Hurbain, P.R.; et al. Optical calibration and equivalence of a multiwavelength thermal/optical carbon analyzer. *Aerosol Air Qual. Res.* **2015**, *15*, 1145–1159. [CrossRef]

45. U.S.EPA, IO Compendium Method IO-3.1: Compendium of Methods for the Determination of Inorganic Compounds in Ambient Air: Selection, Preparation and Extraction of Filter Material, U.S.EPA, Cincinnati, OH. 1999. Available online: https://www.epa.gov/esam/epa-io-inorganic-compendium-method-io-31-selection-preparation-and-extraction-filter-material (accessed on 21 June 2024).
46. U.S.EPA, IO Compendium Method IO-3.4: Compendium of Methods for the Determination of Inorganic Compounds in Ambient Air: Determination of Metals in Ambient Particulate Matter using Inductively Coupled Plasma (ICP) Spectroscopy, U.S.EPA, Cincinnati, OH. 1999. Available online: https://www.epa.gov/amtic/compendium-methods-determination-inorganic-compounds-ambient-air (accessed on 21 June 2024).
47. Ministry of the Environment. Analytical Methods. In *Standard Guidelines for the Environmental Monitoring of Chemicals*; Ministry of the Environment, Government of Japan: Tokyo, Japan, 2002; pp. 41–130.
48. Albero, B.; Tadeo, J.L.; Pérez, R.A. Ultrasound-assisted extraction of organic contaminants. *TrAC Trends Anal. Chem.* **2019**, *118*, 739–750. [CrossRef]
49. Toxicological Profile for Polycyclic Aromatic Hydrocarbons. 1995. Available online: https://www.ncbi.nlm.nih.gov/books/NBK598190/ (accessed on 21 June 2024).
50. Khobragade, P.P.; Ahirwar, A.V. Chemical and morphological characterization of PM2.5 samples collected over an urban industrial region Raipur, Chhattisgarh. *Acta Geophys.* **2023**, *71*, 3057–3076. [CrossRef]
51. Wang, J.; Tu, J.; Lei, H.; Zhu, H. The effect of graphitization degree of carbonaceous material on the electrochemical performance for aluminum-ion batteries. *RSC Adv.* **2019**, *9*, 38990–38997. [CrossRef] [PubMed]
52. Li, C.; Hu, Y.; Chen, J.; Ma, Z.; Ye, X.; Yang, X.; Wang, L.; Wang, X.; Mellouki, A. Physiochemical properties of carbonaceous aerosol from agricultural residue burning: Density, volatility, and hygroscopicity. *Atmos. Environ.* **2016**, *140*, 94–105. [CrossRef]
53. Siddique, R. Wood Ash. In *Waste Materials and By-Products in Concrete*; Springer: Berlin/Heidelberg, Germany, 2008; pp. 303–321. [CrossRef]
54. Morakinyo, O.M.; Mukhola, M.S.; Mokgobu, M.I. Health risk analysis of elemental components of an industrially emitted respirable particulate matter in an urban area. *Int. J. Environ. Res. Public Health* **2021**, *18*, 3653. [CrossRef] [PubMed]

Disclaimer/Publisher's Note: The statements, opinions and data contained in all publications are solely those of the individual author(s) and contributor(s) and not of MDPI and/or the editor(s). MDPI and/or the editor(s) disclaim responsibility for any injury to people or property resulting from any ideas, methods, instructions or products referred to in the content.